Phase diagrams of quasi-binary polymer solutions and blends

Stephen J. Mumby*, Peter Sher and B. E. Eichinger
BIOSYM Technologies Inc., 9685 Scranton Road, San Diego, CA 92121, USA
(Received 4 August 1992; revised 8 October 1992)

A generalized Flory–Huggins theory is presented for use in fitting and predicting liquid–liquid phase diagrams of quasi-binary polymer solutions and blends, in which one component may be polydisperse. A temperature- and concentration-dependent χ parameter is employed. As has been demonstrated previously for simple binary systems, the form chosen for χ is sufficient to fit phase diagrams having upper and lower critical solution temperatures (*UCST* and *LCST*), combination of the two with the *LCST* lying above the *UCST*, closed loop and hour-glass shapes. In extending this work to quasi-binary systems, the phase diagrams obtained are compared with those for binary solutions and blends. It is illustrated how polymer solutions, in which the polymeric component has the same weight-average molecular weight and even the same polydispersity index, although having identical spinodals, may exhibit markedly different cloud-point curves. Comparison is also made with experimental data determined on a model quasi-binary system. Such comparisons may be used to extract the temperature and concentration dependence of χ for the system.

(Keywords: phase diagrams; quasi-binary solutions; quasi-binary blends; interaction parameter; Flory–Huggins theory; modelling)

INTRODUCTION

Phase diagrams are useful in understanding polymer solutions, and they are critical to the proper design of polymer blends. It is known both theoretically and experimentally that the average molecular weight and the molecular-weight distribution can have a significant effect on the location and shape of phase diagrams[1,2]. The effect of molecular-weight distribution on the form of the phase diagrams of quasi-binary polymer solutions has been studied previously in a quantitative manner[3,4]. However, these investigations focused primarily on upper critical solution temperature (*UCST*) phase diagrams. Other types of phase diagrams, such as lower critical solution temperature (*LCST*), combined *LCST* and *UCST*, closed loop and hour-glass, have been observed experimentally for polymer solutions and blends[5,6]. Recently, a modelling method has been described[7,8] that is capable of calculating all these types of phase diagrams for binary polymer solutions and blends. This method is based on a temperature- and composition-dependent χ interaction parameter of the form[7,8]:

$$\chi(T, \varphi_2) = (1 + b_1\varphi_2 + b_2\varphi_2^2)(d_0 + d_1/T + d_2 \ln T) \quad (1)$$

where the coefficients b_i and d_i are adjustable constants. This form of the temperature dependence follows from the assumption that the change in heat capacity upon mixing, Δc_p, is independent of temperature. The quadratic composition dependence was chosen because it has been found to be sufficient to describe most of the experimentally determined χ parameters for solutions[9–11]. Finally, it is assumed that the temperature dependence of χ is uniform for all compositions.

Here, the application of this modelling method to quasi-binary polymer solutions and blends is described, and the critical points, cloud-point curves and spinodal curves are quantitatively investigated.

THERMODYNAMIC QUANTITIES

The Gibbs free-energy density of mixing of component 1 with component 2 of a quasi-binary system (one polydisperse component) is given by:

$$\frac{\Delta G}{RT} = \frac{1 - \varphi_2}{N_1}\ln(1 - \varphi_2) + \sum_{i=1}^{n}\frac{\varphi_{2i}}{N_{2i}}\ln\varphi_{2i} + g(T, \varphi_2)\varphi_2(1 - \varphi_2) \quad (2)$$

The effect of molecular weight on the interaction parameter is typically small[3] and is, therefore, neglected in equation (2). The relative molar volume of component 1 is N_1; N_{2i} and φ_{2i} are the relative molar volume and volume fraction of the ith constituent in component 2; and φ_2 is the total volume fraction of component 2. The interaction parameters $g(T, \varphi_2)$ and $\chi(T, \varphi_2)$ are related by[3,8]:

$$\int_{\varphi_2}^{1}\chi(T, \varphi)\,d\varphi = (1 - \varphi_2)g(T, \varphi_2) \quad (3)$$

Furthermore[8]:

$$\chi'(T, \varphi_2) = 2g'(T, \varphi_2) - (1 - \varphi_2)g''(T, \varphi_2) \quad (4)$$

and

$$\chi''(T, \varphi_2) = 3g''(T, \varphi_2) - (1 - \varphi_2)g'''(T, \varphi_2) \quad (5)$$

Here, the prime, double prime and triple prime denote the first, second and third derivatives of the appropriate

* To whom correspondence should be addressed

0032-3861/93/122540-06

interaction parameter with respect to the volume fraction of component 2.

The chemical potential $\Delta\mu_i$ of the ith constituent in the solution is defined as:

$$\Delta\mu_i = \left.\frac{\partial \Delta G}{\partial n_i}\right|_{T,P,n_j} \tag{6}$$

where n_i is the number of moles of the ith constituent.

The following expressions for the chemical potentials of component 1, $\Delta\mu_1$, and of the ith constituent of component 2, $\Delta\mu_{2i}$, can be derived from equations (2) to (6):

$$\frac{\Delta\mu_1}{RT} = \ln(1-\varphi_2) + \varphi_2\left(1 - \frac{N_1}{N_{2n}}\right) + \chi(T,\varphi_2)N_1\varphi_2^2 \tag{7}$$

$$\frac{\Delta\mu_{2i}}{RT} = \ln\varphi_2 + 1 - \frac{N_{2i}}{N_{2n}}\varphi_2 - \frac{N_{2i}}{N_1}(1-\varphi_2) - N_{2i}\varphi_2(1-\varphi_2)\chi(T,\varphi_2) + N_{2i}\int_{\varphi_2}^{1}\chi(T,\varphi)\,d\varphi \tag{8}$$

where N_{2n} is the number-average relative molar volume of component 2.

PHASE EQUILIBRIA IN QUASI-BINARY SYSTEMS

In binary systems, the binodal represents three different coinciding curves: (i) the locus of the cloud points, (ii) the locus of the incipient phases coexisting with the principal phase that just became clouded, and (iii) the locus of the two coexisting macrophases that develop as the temperature is moved beyond the cloud point. In ternary and higher systems, the binodal becomes a hypersurface in multidimensional T-composition hyperspace that fulfils simultaneously all of the above three functions; however, it is not within our capability to perceive it and make use of it. Typically, phase diagrams of quasi-binary systems employing only two coordinates represent merely a section of the binodal hypersurface, and the various loci mentioned above are projected as different curves: (i) cloud-point curve (*CPC*), (ii) shadow curve and (iii) coexistence curve. The spinodal curve retains the same form and significance for a quasi-binary system as in the true binary case.

Cloud-point curve (CPC)

The *CPC* describes the precipitation temperature, or the χ interaction parameter at this temperature, as a function of solute concentration. Using the calculation method developed by Solc[12], the *CPC* for a quasi-binary system is obtained by solving the following two equations:

$$\tfrac{1}{2}(1+v_0)\sigma + (\mu_{-1} - v_{-1}) + \frac{1}{N_1}(v_0 - 1) + \frac{1}{N_1}\left(\frac{1}{\varphi_2} - \frac{1+v_0}{2}\right)\ln\left(\frac{1-v_0\varphi_2}{1-\varphi_2}\right) + \frac{1}{2}\left((v_0-1)[\chi(T,v_0\varphi_2)(v_0\varphi_2) + \chi(T,\varphi_2)\varphi_2] - (v_0+1)\int_{\varphi_2}^{\varphi_2 v_0}\chi(T,\varphi)\,d\varphi\right) = 0 \tag{9}$$

$$\sigma - \frac{1}{N_1}\ln\left(\frac{1-v_0\varphi_2}{1-\varphi_2}\right) - \left(v_0\varphi_2\chi(T,v_0\varphi_2) - \varphi_2\chi(T,\varphi_2) + \int_{\varphi_2}^{\varphi_2 v_0}\chi(T,\varphi)\,d\varphi\right) = 0 \tag{10}$$

These two equations are essentially equations (8) and (9) of ref. 12. The separation factor σ, as well as the statistical moments ν_k and μ_k ($k = -1, 0$) are defined as[4]:

$$\varphi''_{2i}/\varphi'_{2i} = \exp(\sigma N_{2i}) \tag{11}$$

$$\nu_k = \int N^k w(N)\exp(\sigma N)\,dN \tag{12}$$

and

$$\mu_k = \int N^k w(N)\,dN \tag{13}$$

where φ''_{2i} and φ'_{2i} are the volume fractions of component 2 in the incipient and original-solution phases, and $w(N)$ is the relative molar volume distribution of component 2.

Shadow curve

The shadow curve describes the total concentration of component 2 in the incipient phase, $\varphi_2 v_0$, isothermally phase separated at the cloud point with concentration φ_2. It is obtained from the integrated versions of the cloud-point expressions.

Spinodal

The spinodal curve defines the boundary between unstable and metastable mixtures. Thermodynamically, it is expressed by the determinant[3]:

$$Y = \left|\frac{\partial^2 \Delta G}{\partial\varphi_{2i}\partial\varphi_{2j}}\right| = 0 \tag{14}$$

and the spinodal curve is given explicitly by:

$$\frac{1}{N_1(1-\varphi_2)} - [2\chi(T,\varphi_2) + \varphi_2\chi'(T,\varphi_2)] + \frac{1}{\varphi_2 N_{2w}} = 0 \tag{15}$$

Critical point

The critical point is the point on the cloud-point curve and spinodal curve where the two phases become identical and form one phase. Thermodynamically, it is determined by simultaneously solving equation (14) and the following equation[3]:

$$Y' = 0 \tag{16}$$

where Y' is the determinant derived from equation (14) by replacing the elements of any horizontal line by $\partial Y/\partial\varphi_{21}$, $\partial Y/\partial\varphi_{22}$, etc.* Explicitly, equation (16) is given by

$$-\frac{1}{N_1(1-\varphi_2)^2} + [3\chi'(T,\varphi_2) + \varphi_2\chi''(T,\varphi_2)] + \frac{N_{2z}}{N_{2w}^2\varphi_2^2} = 0 \tag{17}$$

Here N_{2w} and N_{2z} are the weight-average and z-average relative molar volumes of component 2, respectively.

* It is worth noting that equations (14) and (16), which are necessary conditions for the existence of a critical point, do not constitute a sufficient condition when the cofactors of all the elements in the replaced row are 0. See, for example, refs. 13–15

COMPARISON OF PHASE DIAGRAMS OF HYPOTHETICAL BINARY AND QUASI-BINARY SYSTEMS

Solutions of polymers with Schulz–Zimm molecular-weight distributions

To illustrate the versatility of this theoretical approach, and the key differences between phase diagrams of quasi-binary and true binary systems, phase diagrams have been computed for several hypothetical polymer solutions. Polymer solutions having five different χ interaction parameters have been investigated, and the coefficients for the temperature dependence of these interaction parameters are given in *Table 1*. Note that, for simplicity, χ is assumed to be independent of concentration for all these systems. However, the effect of concentration on the phase diagrams can be easily investigated by manipulating the values of the coefficients b_1 and b_2. These five interaction parameters were selected so as to produce phase diagrams of the five types that have been observed experimentally[5,6], i.e. *UCST*, *LCST*, combination of the two with the *LCST* lying above the *UCST*, closed loop and hour-glass. Four sets of polymer solutions were investigated for each of these five χ interaction parameters. All of these solutions comprise a single polymeric component and a low-molecular-weight solvent (M = 100). Both components are assumed to have densities of unity. The polymers in three of the solutions have Schulz–Zimm distributions of molecular weight with identical weight-average molecular weights (M_w = 10 000), but each with a different value of the coupling constant: $k = 1$ (M_n = 5000, M_z = 15 100), $k = 2$ (M_n = 6670, M_z = 13 350), $k = 3$ (M_n = 7500, M_z = 12 500). Physically, the value of k reflects different types of termination mechanisms[16]. The polymeric component in the fourth solution is monodisperse (M = 10 000), and is used for comparison.

The phase diagrams generated using the five χ parameters are shown in *Figures 1–5*. In each of these figures there are up to five curves, or five pairs of curves, depending on the type of phase diagram. In each figure the innermost curve (labelled 's') is the spinodal for all four polymer solutions, the curve labelled 'b' is the binodal for the solution of the monodisperse polymer, and the curves labelled 1–3 correspond to *CPC*s for the solutions of polymers with Schulz–Zimm distributions of molecular weight and k = 1, 2 and 3, respectively. The critical points for the monodisperse polymers in solution are marked (▲) in *Figures 1–5*. Thus, it is clearly illustrated in *Figures 1–5* that, although the spinodals for each of the polymer solutions with the same M_w and χ parameter are identical, their *CPC*s differ substantially. Also, the locations of the critical point(s) for each of these solutions are different. (See *Table 2* for the critical values of concentration, χ parameter and temperature, corresponding to the critical points in *Figures 1–5*.) For the true binary (monodisperse polymer) system the critical points, if any exist, are located at the extrema of the spinodals, which coincide with the extrema of the binodals. For the quasi-binary systems, however, the critical points may be seen to be characteristically offset from the extrema; the critical concentration moves towards a higher concentration of polymer, and the critical temperature either decreases or increases depending upon whether it is located close to a *UCST* or an *LCST*, respectively. Qualitatively, these phenomena are to be expected. From examination of equations (9)–(17), it can be seen that the spinodal depends on M_w, but that the critical point(s) depend(s) on M_w and M_z, and that to describe the *CPC* of a quasi-binary system

Table 1 Coefficients of χ used to generate the phase diagrams shown in *Figures 1–5*

Figure and type	d_0	d_1	d_2
1. *LCST*	0.80	−60.0	0.0
2. *UCST*	0.45	60.0	0.0
3. *LCST* and *UCST*	−0.628	60.0	0.18
4. Closed loop	1.836	−60.0	−0.18
5. Hour-glass	−0.615	60.0	0.18

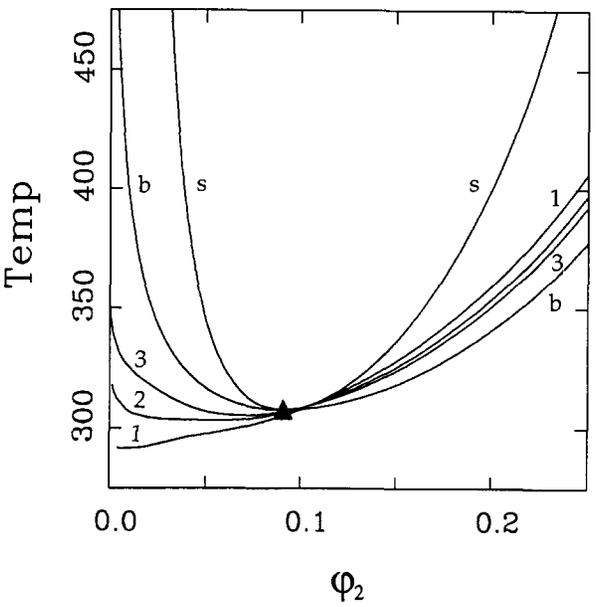

Figure 1 *LCST*-type phase diagram showing the spinodal (s), binodal (b) and critical point (▲) for the monodisperse polymer in solution, and the *CPC*s for the solutions of polymers having Schulz–Zimm distributions of molecular weight and k = 1, 2 and 3

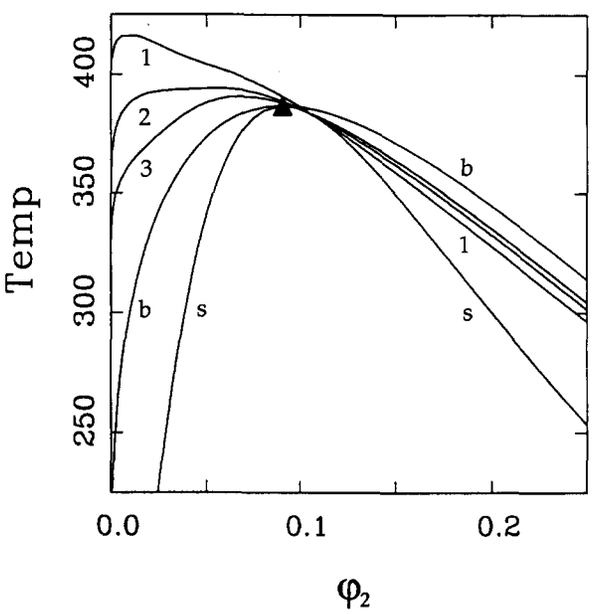

Figure 2 *UCST*-type phase diagram. See caption to *Figure 1* for explanation of curves

requires a knowledge of the details of the molecular-weight distribution.

It has been found previously[17] that a quasi-binary solution containing a polymer with a continuous exponential distribution of molecular weight exhibits a lower compatibility than a binary solution made up of the same solvent and a monodisperse sample of the same polymer whose molecular weight was equivalent to the M_w of the polydisperse component. In contrast, it can be seen from *Figures 1–5* that solutions of a polymer with a Schulz–Zimm distribution of molecular weight show diminished compatibility for volume fractions of polymer, φ_2, lower than the critical volume fraction, φ_2^{crit}, but enhanced compatibility for $\varphi_2 > \phi_2^{crit}$. This effect is most pronounced at the lowest concentrations of polymer, and is accentuated as the polymer becomes more polydisperse (i.e. the value of k is decreased). Indeed, for the polymer solutions corresponding to the phase diagrams in *Figures 3* and *5*, the most polydisperse polymers (lowest k) are completely immiscible with the solvent at low polymer concentrations over the entire temperature range plotted. Furthermore, the effect observed in *Figure 3* is so great that, for the solution containing the most polydisperse polymer ($k = 1$), the combined *UCST/LCST CPCs* have now coalesced to form an hour-glass-type *CPC*. This is despite the fact that the spinodals remain unchanged in the combined *UCST/LCST* form. Thus, the termination mechanism of a polymerization reaction affects the location of the critical points and the shape of the *CPCs* of solutions of the resulting polymer, and consequently influences the degree of miscibility in these systems.

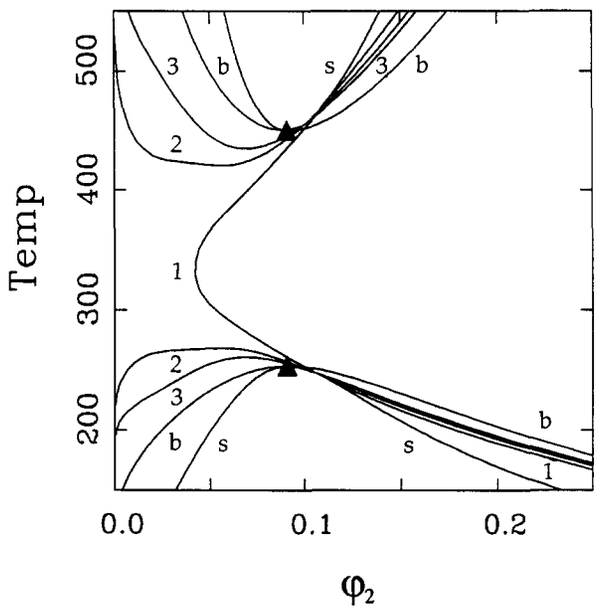

Figure 3 Combined *LCST*- and *UCST*-type phase diagram. See caption to *Figure 1* for explanation of curves

Solutions of polymers with the same polydispersity index

As a further example of the effect of polydispersity on *CPCs*, three polymer solutions are considered, each comprising a low-molecular-weight solvent ($M = 100$)

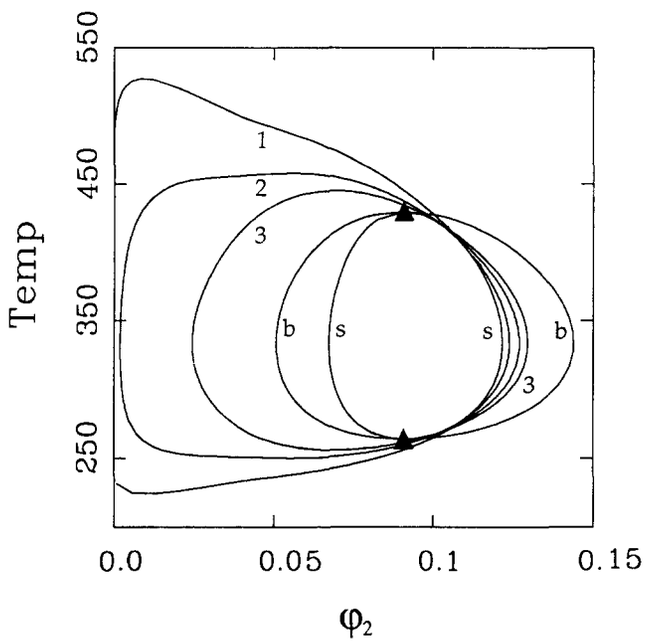

Figure 4 Closed-loop-type phase diagram. See caption to *Figure 1* for explanation of curves

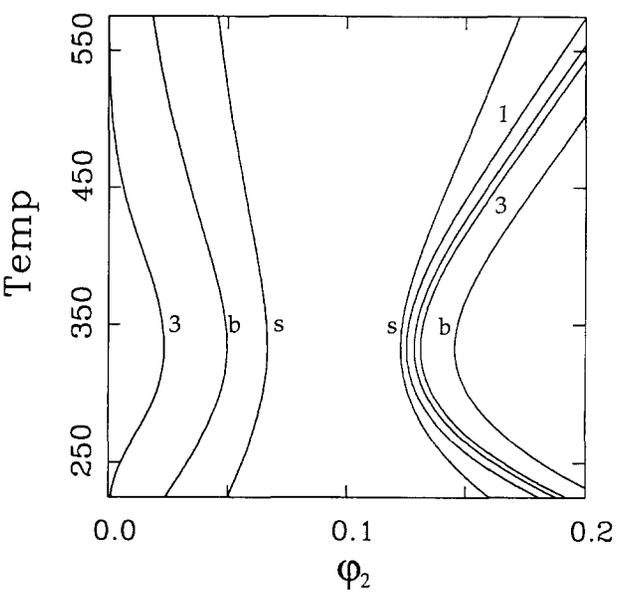

Figure 5 Hour-glass-type phase diagram. See caption to *Figure 1* for explanation of curves. No critical points exist for these systems in the range plotted

Table 2 Critical values of the volume fraction of polymer, φ_2^{crit}, interaction parameter, χ^{crit}, and temperature, T^{crit}

			T^{crit} (K)					
	φ_2^{crit}	χ^{crit}	Fig. 1	Fig. 2	Fig. 3		Fig. 4	
Monodisperse	0.0910	0.6050	307.7	387.1	253.7	450.0	263.7	429.8
$k = 1$	0.1092	0.6070	310.9	382.1	245.3	469.2	276.7	406.5
$k = 2$	0.1035	0.6060	309.3	384.5	249.3	459.8	269.8	418.5
$k = 3$	0.1006	0.6056	308.7	385.6	251.0	455.9	267.3	423.1

and a polydisperse polymer ($M_w = 10000$, $D = 2.0$). Although all of the polymer components have identical weight-average molecular weights, M_w, and polydispersity indices, D ($= M_w/M_n$), the actual molecular-weight distributions of these components are different. Specifically, the distributions are Flory, quasi-log-normal, and a discrete mixture of two monodisperse polymers (90% of the number of molecules with a molecular weight of $M = 3333$, and 10% with $M = 20000$). The first χ parameter from *Table 1* was

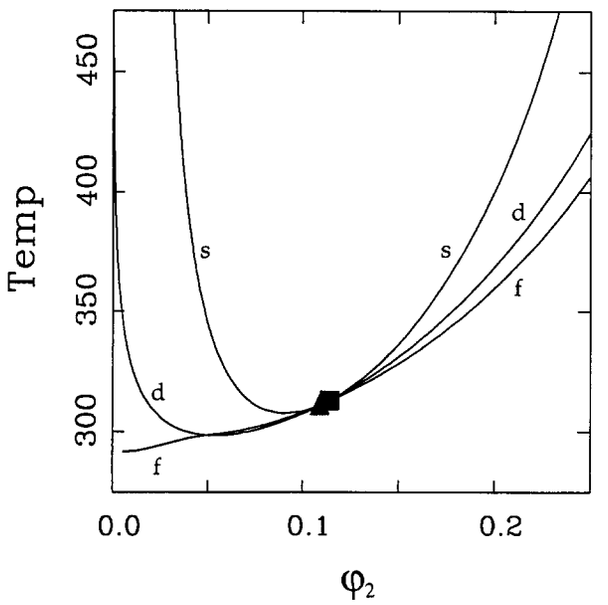

Figure 6 *LCST*-type phase diagram. The polymers in the two solutions have the same weight-average molecular weight and polydispersity index, but different molecular-weight distributions. Shown are the spinodal (s), and the *CPCs* for the solutions of polymers having discrete (d, c.p. = ■) and Flory (f, c.p. = ▲) distributions of molecular weight

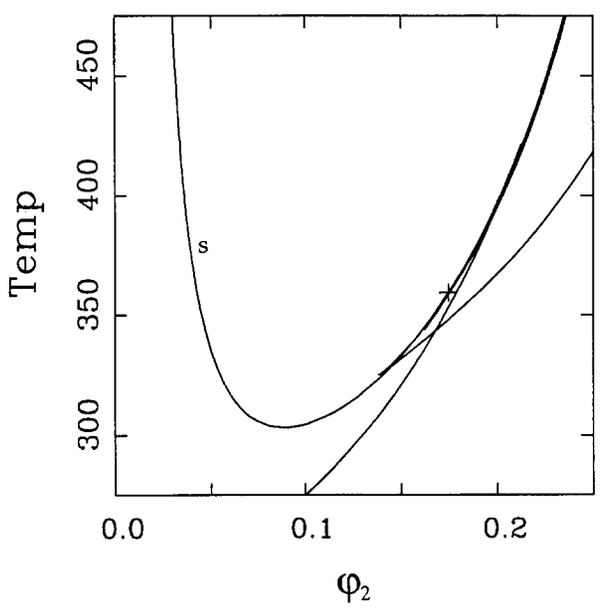

Figure 7 The *LCST* phase diagram shown here is also for a solution of a polymer with the same weight-average molecular weight and polydispersity index as for those corresponding to the phase diagram in *Figure 6*, but with a quasi-log-normal distribution of molecular weight. The critical point (+), spinodal (s) and the *CPC* are shown

then used to generate the *LCST*-type phase diagrams shown in *Figures 6* and *7*.

In *Figures 6* and *7*, the innermost curve ('s') is the spinodal for all the systems. Also shown in *Figure 6* are the *CPCs* of the Flory ('f'), and the mixture of the two monodisperse components ('d'), as well as the critical points (▲, ■) for these solutions. The solution containing the polymer with the Flory molecular-weight distribution displays a lower compatibility than that containing the discrete mixture for all volume fractions of polymer greater than the critical concentration. This is also true at very low concentrations of polymer, and here the difference in compatibility is most pronounced. However, for polymer concentrations just less than the critical value, although differences are slight, the opposite may be seen to be true.

In *Figure 7*, in addition to the spinodal, the *CPC* for the solution containing the polymer with a quasi-log-normal molecular-weight distribution and the critical point (+) for this system are shown. The *CPC* for this solution is markedly different from any of those shown in *Figure 6*. In particular, this *CPC* exhibits a depression close to the critical point, and a triple point at which two incipient phases of different composition are at equilibrium with the principal phase. This behaviour has been discussed in detail[18,19] for a *UCST* phase diagram of a solution containing a polymer with a true log-normal molecular-weight distribution, and has been attributed to the presence of a minute but significant amount of a very high-molecular-weight material. Indeed, depressions of this type have been observed experimentally[20] in *CPCs* for mixtures of epoxy monomers of the DGEBA type (diglycidyl ether of bisphenol A) with CTBN (carboxyl-terminated butadiene–acrylonitrile random copolymer) rubbers.

These figures illustrate very clearly that polymer solutions in which the polymeric components have the same values of M_w and D may still exhibit significantly different *CPCs*. An *LCST*-type phase diagram was selected to illustrate this point; however, the effects described occur regardless of the type of phase diagram. Thus, in order to compare quantitatively *CPCs* of different quasi-binary polymer systems, a knowledge of the details of the molecular-weight distributions of the polymeric components is required.

COMPARISON WITH EXPERIMENTAL DATA

Few experimental data are available in the literature of *CPCs* for quasi-binary polymer solutions or blends for which the details of the molecular-weight distributions of the polymeric components have been carefully characterized. However, Tong *et al.*[21] performed measurements on three model polymer mixtures that were prepared by mixing four narrow molecular-weight distribution polystyrene fractions in different ratios. The weight-average molecular weight and polydispersity index of these four fractions (F1, F2, F3, F4) are listed in *Table 3*, and the composition by weight of the three mixtures (M1, M2, M3) of these fractions is given in *Table 4*. The experimental *CPCs* of the three mixtures in cyclohexane are replotted as the symbols in *Figure 8*. Using the distributions of molecular weight given in *Table 4*, theoretical *CPCs* were fitted to the experimental data, and the results are shown as curves in the same figure. The fitting was performed to all three experimental *CPCs*

Table 3 Weight-average molecular weight and polydispersity of the polystyrene fractions[21]

Fraction	M_w	M_w/M_n
F1	11 000	1.02
F2	44 500	1.01
F3	195 000	1.07
F4	807 000	1.01

Table 4 Composition by weight of the polystyrene mixtures[21]

Mixture	M1	M2	M3
F1	0.4	0.25	0.1
F2	0.3	0.25	0.2
F3	0.2	0.25	0.3
F4	0.1	0.25	0.4
M_w	137 500	264 400	391 300
M_w/M_n	6.08	7.92	6.11

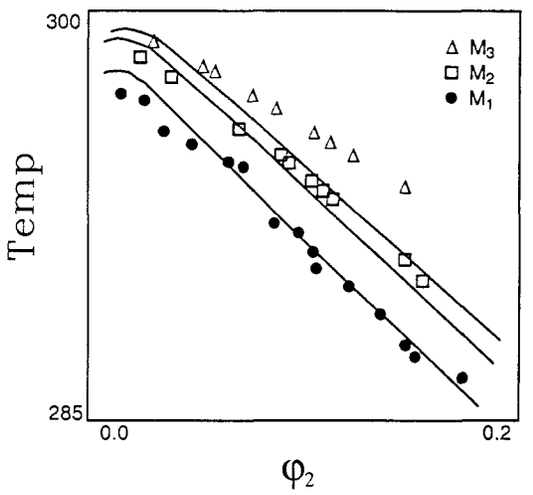

Figure 8 Experimental data from ref. 21 and theoretically fitted *CPC*s for solutions of polystyrene in cyclohexane

simultaneously, so that a single χ interaction parameter was obtained as:

$$\chi = -1.149 + 500/T$$

Unfortunately, it was not found possible to obtain a good fit to all three *CPC*s simultaneously. Even by using non-zero values of the coefficients b_1 and b_2 in equation (1) to introduce composition dependence into χ, the quality of the fit to the experimental data could not be appreciably enhanced. In *Figure 8*, it can be seen that, although the theoretical *CPC* produced using the χ parameter above is in good agreement with the experimental data for the solution containing the polystyrene blend with the lowest M_w, the quality of the agreement decreases as the M_w of the system increases. This implies an apparent molecular-weight dependence of χ for this system, and the enhanced Flory–Huggins theory described here assumes χ to be independent of molecular weight. Virial theories would give rise to a molecular-weight dependence through the second virial coefficient. However, no such theory is yet available that can produce quantitative agreement with experimental data. Fortunately, for most polymer solutions and blends χ is not strongly dependent upon molecular weight[8], and the theory presented here gives a good description of the liquid–liquid phase behaviour. For the polystyrene/cyclohexane system, good fits could be readily achieved to each of the *CPC*s individually. However, this would, of course, result in several χ parameters.

CONCLUSION

A temperature- and concentration-dependent interaction parameter has been used to study liquid–liquid phase diagrams of quasi-binary polymer solutions and blends in which one component may have a molecular weight distribution. This approach can be used to generate the five most generally observed types of phase diagrams. Polymer solutions in which the polymeric component has the same weight-average molecular weight, and even the same polydispersity index, may have markedly different cloud-point curves. Thus, in order to compare quantitatively the cloud-point curves for different polymer samples in a quasi-binary system, it is necessary to know the exact molecular-weight distribution of the polymer. The interaction parameter of a polymer solution or a blend is obtained when a best fit between the theoretically and experimentally determined values is obtained.

ACKNOWLEDGEMENTS

The authors gratefully acknowledge beneficial discussions with Dr Karel Solc. This work was supported as part of Biosym Technologies' Polymer Project, which is funded by a consortium of 50 companies and government laboratories.

REFERENCES

1 Tompa, H. *Trans. Faraday Soc.* 1949, **45**, 1141
2 Flory, P. J. 'Principles of Polymer Chemistry', Cornell University Press, Ithaca, NY, 1953
3 Koningsveld, R. *J. Polym. Sci. (A-2)* 1968, **6**, 305 and 325
4 Solc, K. *Macromolecules* 1970, **3**, 665
5 Siow, K. S., Delmas, G. and Patterson, D. *Macromolecules* 1972, **5**, 29
6 Ougizawa, T., Inoue, T. and Kammer, H. W. *Macromolecules* 1985, **18**, 2089
7 Qian, C., Mumby, S. J. and Eichinger, B. E. *Polym. Prepr.* 1990, **31** (2), 621, 691
8 Qian, C., Mumby, S. J. and Eichinger, B. E. *Macromolecules* 1991, **24**, 1655
9 Orwoll, R. J. *Rubber Chem. Technol.* 1977, **452**, 50
10 Barton, A. F. M. 'Handbook of Solubility Parameters and Other Cohesion Parameters', CRC Press, Boca Raton, FL, 1983
11 Barton, A. F. M. 'Handbook of Polymer–Liquid Interaction Parameters and Solubility Parameters', CRC Press, Boca Raton, FL, 1990
12 Solc, K., Kleintjens, L. A. and Koningsveld, R. *Macromolecules* 1984, **17**, 573
13 Solc, K. and Koningsveld, R. *J. Phys. Chem.* 1985, **89**, 2237
14 Bergmann, J., Kehlen, H. and Ratzsch, M. T. *J. Macromol. Sci. Chem.* 1988, **A25**, 1127
15 Brannock, G. R. *J. Chem. Phys.* 1991, **95**, 612
16 Munk, P. 'Introduction to Macromolecular Science', Wiley, New York, 1989, p. 89
17 Koningsveld, R., Kleintjens, L. A. and Schoffeleers, H. M. *Pure Appl. Chem.* 1974, **39**, 1
18 Solc, K. *J. Polym. Sci., Polym. Phys. Edn.* 1974, **12**, 555
19 Solc, K. *Macromolecules* 1975, **8**, 819
20 Verchere, D., Sautereau, H., Pascault, J. P., Moschiar, S. M., Riccardi, C. C. and Williams, R. J. J. *Polymer* 1989, **30**, 107
21 Tong, Z., Einaga, Y. and Fujita, H. *Macromolecules* 1985, **18**, 2264